EPJ Web of Conferences **71**, 00053 (2014)
DOI: 10.1051/epjconf/20147100053

Rare Decays at LHCb

Sam Hall[1,a] on behalf of the LHCb collaboration

[1] *Imperial College London*

Abstract. Rare decays of beauty and charm hadrons provide an effective method of testing the Standard Model and probing possible new physics scenarios. The LHCb experiment has published a variety of interesting results in this field, some of which are presented here. In particular the measurements of the branching fractions of $B^0_{(s)} \to \mu^+\mu^-$ which, in combination with CMS, resulted in the first observation of the $B^0_s \to \mu^+\mu^-$ decay. Other topics include searches for the rare decay $D^0 \to \mu^+\mu^-$, the lepton flavour violating decays $B^0_{(s)} \to e^\pm\mu^\mp$, and the observation of the $\psi(4160)$ resonance in the region of low recoil in $B^+ \to K^+\mu^+\mu^-$ decay. New results on the angular analysis of the decay $B^0 \to K^{*0}\mu^+\mu^-$ with form factor independent observables are also shown.

1 Introduction

Flavour changing neutral currents (FCNCs) are forbidden at tree level in the Standard Model (SM) and thus are mediated by loop processes. At leading order these loops are either penguin or box type diagrams, Fig. 1a. Virtual particles can enter these loops, probing mass scales much higher than those accessible via direct production. In the SM $b \to s$ transition the t-quark dominates in the loop, but in a New Physics (NP) model such as Supersymmetry (SUSY) other heavy particles, see Fig. 1b, can contribute and significantly alter the observed physics. These indirect probes are complementary approaches to those taken by general purpose detectors.

The rare nature of the aforementioned transitions is exploited as a tool for hunting NP since contributions could be of the same order to those from the SM. A FCNC decay's suppression is dependent on a number of factors, particularly the mass of the quark mediating the loop, the GIM mechanism and helicity suppression.

Measurements of rare decays strongly constrain possible new physics scenarios in a model independent way using the Operator Product Expansion (OPE). The OPE uses an effective Hamiltonian with all heavy fields, such as the top and W, integrated out, it includes a set of generic operators, O_i, and coefficients, C_i, which are known as Wilson coefficients. The operators and Wilson coefficients describe

[a] e-mail: shall@cern.ch

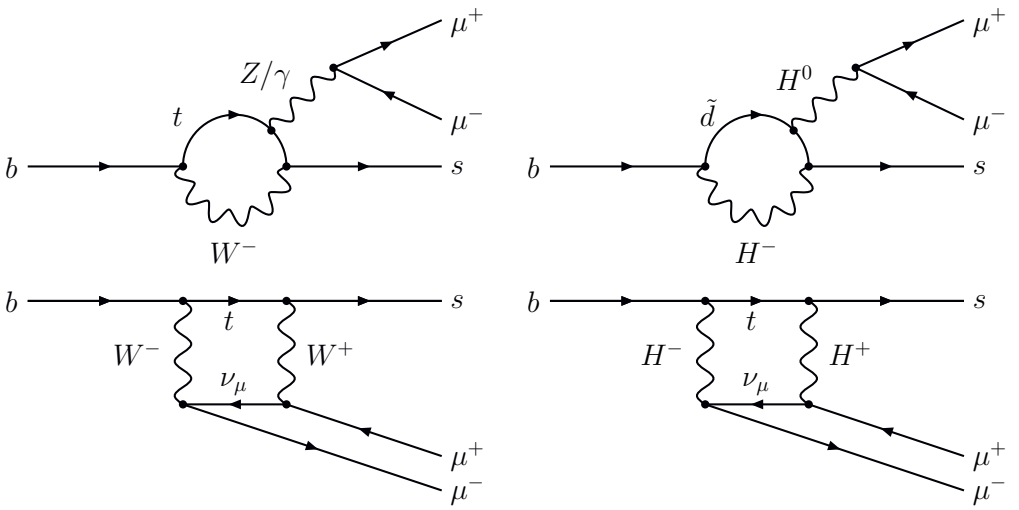

Figure 1: Feynman diagrams showing examples of the $b \to s$ FCNC in the (a) SM and (b) SUSY particles mediating the (top) penguin, (bottom) box loops.

long and short distance interactions respectively, for a $b \to s(d)$ transition the effective Hamiltonian is:

$$\mathcal{H}_{\text{eff}} \approx -\frac{4G_F}{\sqrt{2}} V_{tb} V^*_{ts(d)} \frac{e^2}{16\pi^2} \sum_{i=7,9,10,S,P} (C_i O_i + C'_i O'_i) + \text{h.c.}. \tag{1}$$

In the SM the process is sensitive to the Wilson coefficients C_7, the photonic penguin, C_9, the vector mediated dilepton-penguin, and C_{10} which is the axial-vector mediated dilepton-penguin. The scalar, C_S, and pseudoscalar, C_P, transitions are also included but are suppressed by $m_\ell m_b / m_W^2$. The helicity state disfavoured by the SM is denoted by O'_i and C'_i, these are vanishingly small.

Wilson coefficients are accessible both by measuring branching fractions and angular observables of decaying mesons. Since each Wilson coefficient describes a particular interaction, placing limits on them constrains NP contributions in that process.

Branching fraction measurements and angular distributions of decaying mesons (with interesting helicity structures) lead to direct constraints on all the involved coefficients, and thus potential NP models.

1.1 The LHCb detector

The LHCb experiment is located on the LHC accelerator at CERN and is supplied with pp collisions at $\sqrt{s} = 7(8)$ TeV in 2011(2012). A large $b\bar{b}$ cross-section at these energies in the LHCb acceptance region, $\sigma(b\bar{b}) = (75.3 \pm 14.0)$ μb, [1] means there is an unprecedented number of b-meson and baryon

decays to be analysed. On the other hand, understanding the complex event structure in pp collisions is challenging.

The LHCb detector is a single-arm forward spectrometer covering the pseudorapidity range $2 < \eta < 5$ designed for the study of particles containing b or c quarks. In order to do this effectively the detector is equipped with two Ring Imaging CHerenkov (RICH) detectors. The RICH detectors together with tracking stations, calorimeters and muon chambers gives LHCb excellent particle identification capabilities over the momentum range 1 to 100 GeV/c. For example, the muon identification efficiency is 97% for only a 1 to 3% misidentification rate, and the kaon identification is 95% for only a 5% pion misidentification probability. A silicon-strip VErtex LOcator, VELO, provides high precision track measurements close to the interaction point, giving an impact parameter resolution of 20 μm for tracks with large transverse momentum. A full description of the LHCb detector is given in Ref. [2].

2 Searches for very rare and forbidden decays

Comparable strategies are employed in all rare decay analyses. Signal and normalization candidates are selected by a hardware trigger and subsequent software triggers [3]. Triggers require that there are high p_{T} tracks in an event, and a well defined displaced secondary vertex with reference to the primary vertex defined by the pp collision. Muons in the decay are must register hits in the muon systems.

The complex event structure of pp collisions and the rarity of these events leads to the use of advanced analytical techniques such as multivariate selections. Boosted Decision Trees (BDTs) are the type of favoured multivariate classifier used in these analyses, they are trained to differentiate between signal and background candidates. Input variables are a variety of geometric and kinematic variables. Most background removal is done by placing a cut on the output of the BDT discriminant.

2.1 Analysis of the very rare decay $\mathbf{B^0_{(s)} \to \mu^+\mu^-}$

The decays $B^0_s \to \mu^+\mu^-$ and $B^0 \to \mu^+\mu^-$ are well motivated by theory and LHCb offers an excellent arena to search for them. The decay $B^0_s \to \mu^+\mu^-$ is heavily suppressed in the SM because it is an FCNC, Fig. 1a, and helicity suppressed decays. The $B^0 \to \mu^+\mu^-$ decay is further disfavoured because the FCNC is a $b \to d$ transition, and is therefore rarer by approximately a factor of $|V_{td}/V_{ts}|^2$ in the SM.

There are precise predictions for the branching fraction of these decays in the SM [4]:

$$\begin{aligned} \mathcal{B}(B^0_s \to \mu^+\mu^-) &= (3.23 \pm 0.27) \times 10^{-9}, \\ \mathcal{B}(B^0 \to \mu^+\mu^-) &= (1.07 \pm 0.10) \times 10^{-10}. \end{aligned} \tag{2}$$

Here, branching fraction uncertainties are dominated by the B_s decay constant and the relevant CKM matrix elements.

New scalar, pseudoscalar, and axial-vector particles can all contribute to the loop amplitude; although the axial-vector is helicity suppressed. This would be observed as a deviation in the branching fraction from the SM predictions in Eq. 2. These decays are particularly sensitive to supersymmetry for two main reasons: firstly a neutral Higgs lifts the helicity supression; and secondly the branching fraction is proportional to $\tan^6\beta$, where $\tan\beta$ is the ratio of vacuum expectations values of the up and down components of the SUSY Higgs doublet.

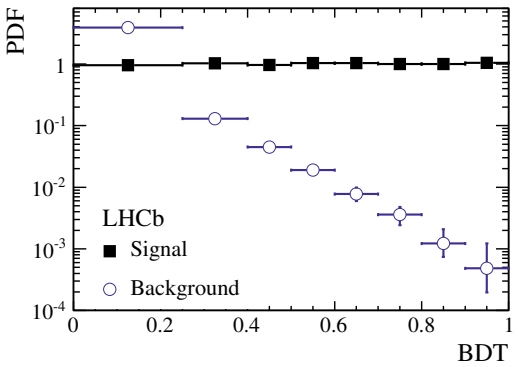

Figure 2: Distributions in bins of the BDT classifier for signal-proxy $B^0_{(}s) - > hh'(h^{(}\prime) = \pi^{\pm}, K^{\pm})$ candidates and for events in the mass sidebands [7]. The signal response is linear whereas the background sample response drops as the BDT value increases.

The ratio of the branching fractions of the decays $B^0_s \to \mu^+\mu^-$ and $B^0 \to \mu^+\mu^-$ leads to some uncertainties being cancelled:

$$\frac{\mathcal{B}(B^0_s \to \mu^+\mu^-)}{\mathcal{B}(B^0 \to \mu^+\mu^-)} = 30.35\,(1 \pm 0.06 \pm 2\sigma_{f_{s/d}}), \tag{3}$$

here $\sigma_{f_{s/d}}$ is the relative error of f_{B_s}/f_{B_d} [4]. This is also a very precise test of the Minimal Flavour Violation, MFV, scenario which assumes that the flavour structure BSM is the same as in the SM, and would therefore be an interesting future measurement for the LHCb upgrade.

Dominant backgrounds for $B^0_{(s)} \to \mu^+\mu^-$ are of the form $b\bar{b} \to X\mu\mu$, caused when a $b\bar{b}$ pair hadronizes separately and decays into final states containing muons appearing to point to a common secondary vertex. Analysis of the decays $B^0_{(s)} \to \mu^+\mu^-$ features two multivariate classifiers. The first, described in Ref. [5], efficiently removes background contamination from $b\bar{b} \to X\mu\mu$ leaving signal efficiency high. Remaining candidates are binned according to the result of the second discriminant thus allowing access to signal candidates that would be removed by a simple cut. The second BDT includes the input variables: B candidate decay time, IP and p_{T}; the minimum χ^2_{IP} of the two muons with respect to any PV; the distance of closest approach between the two muons; and the cosine of the angle between the muon momentum in the dimuon rest frame and the vector perpendicular to both the B candidate momentum and the beam axis. Moreover two different measures for the isolation of signal candidates are included: the number of good two-track vertices a muon can make with other tracks in the event; and the B candidate isolation, introduced in Ref. [6]. The signal efficiency is linear with the value of the BDT cut but the background efficiency drops, Fig. 2. A simultaneous fit is then performed to all bins and the total signal yield extracted.

In the final selection combinatorial background dominates around the B^0_s mass, but peaking background from $B^0_{(}s) - > hh'$, where both hadrons are misidentified as muons. A wrong mass hypothesis here induces a displacement to lower mass and hence only the B^0 mass window is affected. This adds to the challenge of understanding the latter decay.

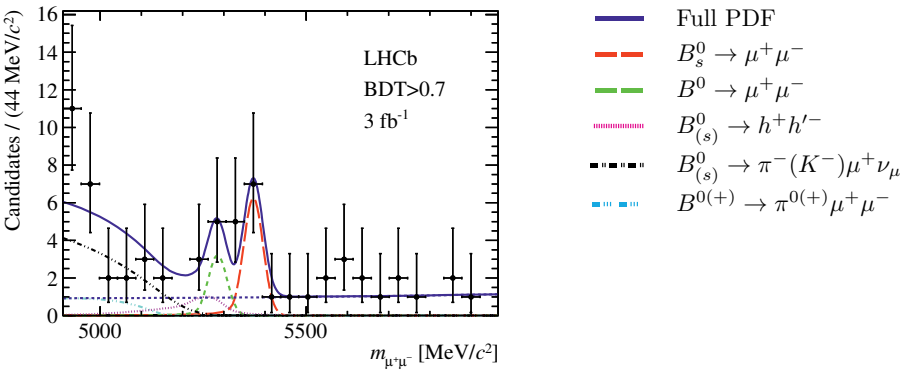

Figure 3: (left) The three most signal like BDT bins are plotted and fitted functions are overlayed.

The normalization is achieved using two decays channels chosen for their similarity to the signal. The decay $B^0 \to K^+\pi^-$ is chosen because it has similar kinematics, and the decay $B^+ \to J/\psi K^+$ where $J/\psi \to \mu^+\mu^-$ is also used because the muon triggering is similar. Signal yield of the normalization and signal channels is used to calculate the branching fractions of $B^0_{(s)} \to \mu^+\mu^-$ using:

$$\mathcal{B}(B^0_q \to \mu^+\mu^-) = \mathcal{B}_{\text{norm}} \cdot \frac{\epsilon_{\text{norm}}}{\epsilon_{B^0_q \to \mu^+\mu^-}} \cdot \frac{f_{\text{norm}}}{f_{B_q}} \cdot \frac{N_{B^0_q \to \mu^+\mu^-}}{N_{\text{norm}}}. \tag{4}$$

In this equation ϵ is the total efficiency of the given decay, this includes the trigger, geometric acceptance and selection. Lastly, f_X denotes a fragmentation function, which is the probability for a b to hadronize into a given hadron X. The values of the fragmentation fractions, f_X, used were measured by LHCb [8].

After normalization, the calculated branching fractions are:

$$\begin{aligned}\mathcal{B}(B^0_s \to \mu^+\mu^-) &= \left(2.9\,^{+1.1}_{-1.0}(\text{stat})\,^{+0.3}_{-0.1}(\text{syst})\right) \times 10^{-9},\\ \mathcal{B}(B^0 \to \mu^+\mu^-) &= \left(3.7\,^{+2.4}_{-2.1}(\text{stat})\,^{+0.6}_{-0.4}(\text{syst})\right) \times 10^{-10},\end{aligned} \tag{5}$$

with statistical significances of 4.0σ and 2.0σ respectively [7]. Low significance of the latter motivates calculating a limit:

$$\mathcal{B}(B^0_d \to \mu^+\mu^-) < 7.4 \times 10^{-10} \tag{6}$$

to 95% confidence level using the CL_s method[9].

The CMS collaboration also published measurements of the branching fractions of these decays [10]. An average of the results from LHCb and CMS has been performed [11], the resulting branching fractions are:

$$\begin{aligned}\mathcal{B}(B^0_s \to \mu^+\mu^-) &= (2.9 \pm 0.7) \times 10^{-9},\\ \mathcal{B}(B^0 \to \mu^+\mu^-) &= \left(3.6\,^{+1.6}_{-1.4}\right) \times 10^{-10}.\end{aligned} \tag{7}$$

The statistical significance of the measurement of $\mathcal{B}(B^0_s \to \mu^+\mu^-)$ is over 5σ, and thus an observation can be claimed. Comparisons of measurements and the combination can be seen in Fig. 4.

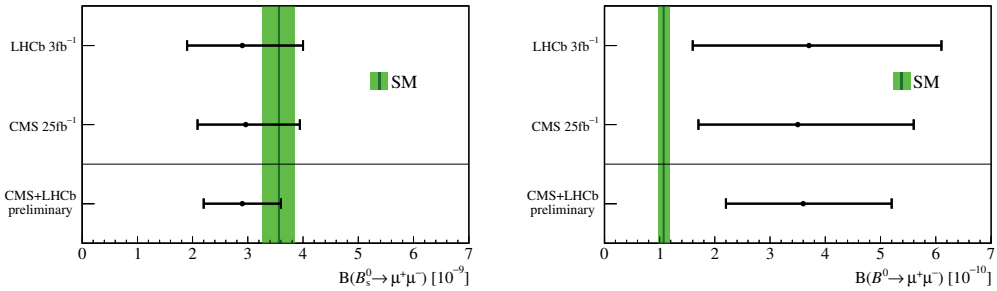

Figure 4: Comparisons of the SM expected branching fraction (green band) for $B_s^0 \to \mu^+\mu^-$ and $B^0 \to \mu^+\mu^-$ with the measurements from CMS, LHCb and the combination of these results (1σ uncertainties are shown). While $\mathcal{B}(B_s^0 \to \mu^+\mu^-)$ is very consistent with the SM, for the B^0 channel the results are still statistically consistent but also slightly enhanced.

The two branching fractions measurements of $B_s^0 \to \mu^+\mu^-$ and $B^0 \to \mu^+\mu^-$ are powerful constraints on NP, particularly SUSY. Considering them alone is enough to remove a large amount of available parameter space for SUSY, which continues to shrink around SM expectations. It also sets constraints on Wilson coefficients, which remain in good agreement with SM predictions as shown in Ref. [12], and for 2012 results Ref. [13].

Although the significance of the measurements of $\mathcal{B}(B^0 \to \mu^+\mu^-)$ from LHCb and CMS are low, they are both above SM predictions, Fig. 4; consequently there has been much interest in the possibility of an enhancement here [14, 15].

2.2 Search for the very rare decay $\mathbf{D^0 \to \mu^+\mu^-}$

The decay $D^0 \to \mu^+\mu^-$ is a $c \to u$ FCNC transition, and therefore more suppressed than a $b \to s$ current because the decay amplitude is proportional to the mass of the quark running in the loop, and $m_t^2 \gg m_b^2$. When there are down-type quarks running in the loops, the GIM mechanism is more effective because they are more degenerate in mass than u-type quarks.

Theoretical predictions are less accurate for the D^0 decay than for the B^0 because long distance effects are dominant. However, there are theoretical predictions of the order [16]

$$\mathcal{B}(D^0 \to \mu^+\mu^-) \simeq 3 \times 10^{-13}, \tag{8}$$

while the previous limit from Belle [17] is:

$$\mathcal{B}(D^0 \to \mu^+\mu^-) < 1.4 \times 10^{-7} \text{at } 90\% \text{ CL}. \tag{9}$$

So, there are approximately six orders of magnitude to explore for possible NP contributions.

The decay $D^0 \to \mu^+\mu^-$ is not sensitive to SUSY theories unless they permit R-parity violation. Many other models can alter the branching fraction; Ref. [18] shows that a new scalar or boson contributing to the decay can modify the total branching fraction proportionally to the mass of the new particle to the power negative four.

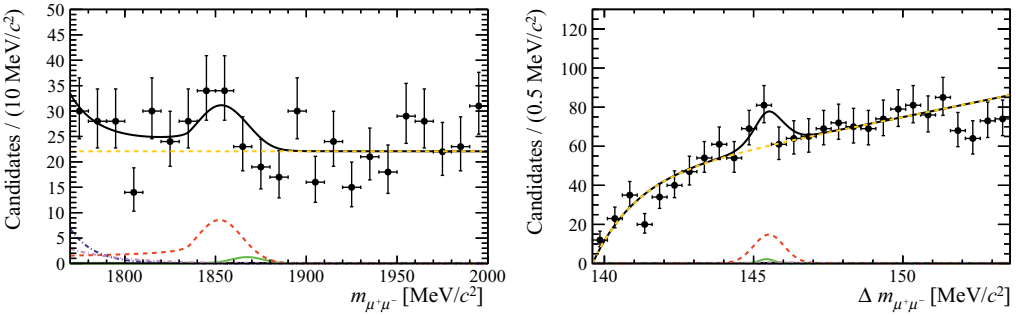

Figure 5: (a) Invariant mass distribution, $m_{\mu\mu}$, with $144 < \Delta m_{\mu\mu} < 147\,\mathrm{MeV}/c^2$ (b) Delta mass distribution where $1820 < m_{\mu\mu} < 1885\,\mathrm{MeV}/c^2$. The fitted pdfs are overlaid, these are: (solid black) the full pdf, (dashed red) $D^0 \to \pi^+\pi^-$, (dashed yellow) combinatorial background, (dash-dotted blue) $D^0 \to K^-\pi^+$, (dash-dotted purple) $D^0 \to \pi^-\mu^+\nu_\mu$.

This analysis uses $1\,\mathrm{fb}^{-1}$ of data collected by LHCb in 2011. The D^0 candidates were selected from reconstructed $D^{*+} \to D^0\pi^+$ requiring a well defined primary and secondary vertices. Again a multivariate selection is applied, optimized to achieve the best possible limit by assuming that no signal will be observed. Yields are extracted from a fit to data in two dimensions, the dimuon mass spectrum $m_{\mu\mu}$, and the difference in mass between the D^{*+} and the D^0, $\Delta m_{\mu\mu}$ [19], the resulting fits are shown in Fig. 5. Normalization is done in relation to the decay $D^0 \to \pi^+\pi^-$ in the same way as shown in Eq. 4. The branching fraction of the normalization mode is $O(10^{-4})$ and this channel also constitutes the main peaking background because of similarity in mass between pions and muons. Studies were done regarding this peaking background, its shape is fixed in the fit. Another background, that appears at lower mass, is from $D^0 \to \pi^-\mu^+\nu_\mu$ where the neutrino is not reconstructed. These backgrounds can all be seen in Fig. 5.

2.3 Search for the forbidden decay $\mathbf{B^0_{(s)} \to e^\pm\mu^\mp}$

The analysis of the decay $B^0_{(s)} \to e^\pm\mu^\mp$ is a direct search for a Lepton Flavour Violation (LFV). Many models permit these kind of interactions, for example heavy singlet Dirac neutrinos [20] can mediate these currents, as could various SUSY models [21]. There are also models which contain leptoquark objects that carry both colour and lepton flavour but many of these conflict with the lifetime of the proton, which is known to be greater than $O(10^{34})$ years, unless the leptoquark is high enough [22]. However, the Pati-Salam model [23] treats lepton number as a fourth colour and predicts $\tau_p \sim 10^{35}$ years and is therefore attractive among these models. Previous limits of lepto-quark masses are set by ATLAS [24–26] and CMS [27–29].

The analysis strategy is very similar to that for $B^0_s \to \mu^+\mu^-$ and $B^0 \to \mu^+\mu^-$ in that there are two BDTs of which a loose cut is applied to one and the remaining candidates are binned in the other. There is then a simultaneous fit to eight BDT bins, each of which contributes equally to the total signal yield. For $B^0_{(s)} \to e^\pm\mu^\mp$ only the normalization channel $B^+ \to K^+\pi^-$ is required and corrections are made for energy losses in bremsstrauhlung from the electron.

No evidence for the decay $B_s^0 \to e^\pm\mu^\mp$ or $B^0 \to e^\pm\mu^\mp$ is seen, and limits on the branching fractions are set:

$$\begin{aligned}\mathcal{B}(B_s^0 \to e^\pm\mu^\mp) &< 1.1(1.4) \times 10^{-8},\\ \mathcal{B}(B^0 \to e^\pm\mu^\mp) &< 2.8(3.7) \times 10^{-9}\end{aligned} \tag{10}$$

at a 90 (95)% confidence level [30]. Model-independant limits on the branching fractions can be interpreted in the context of Pati-Salam lepto-quarks and limits computed on their mass:

$$\begin{aligned}M_{LQ}(B_s^0 \to e^\pm\mu^\mp) &> 107(101)\,\mathrm{TeV}/c^2,\\ M_{LQ}(B^0 \to e^\pm\mu^\mp) &> 135(126)\,\mathrm{TeV}/c^2\end{aligned} \tag{11}$$

at a 90(95)% confidence level [30]. The magnitude of the masses of these particles testifies as to how effective indirect searches for NP are.

3 Electroweak penguin decays

3.1 Observation of a new resonance in $\mathbf{B^+ \to K^+\mu^+\mu^-}$ decay at low recoil

There has been significant interest in measurements of the decay $B^+ \to K^+\mu^+\mu^-$ and $B^0 \to K^0\mu^+\mu^-$ because of the large deviation from SM expectation observed in the Isospin Asymmetry, A_I, of this decay [31]. The A_I is defined as the ratio of the differences in the branching fraction of the neutral and charged modes of $B \to K\mu\mu$ to the sum of them (corrected for lifetime differences):

$$A_I = \frac{\mathcal{B}(B^0 \to K^0\mu^+\mu^-) - \frac{\tau_0}{\tau_+}\mathcal{B}(B^+ \to K^+\mu^+\mu^-)}{\mathcal{B}(B^0 \to K^0\mu^+\mu^-) + \frac{\tau_0}{\tau_+}\mathcal{B}(B^+ \to K^+\mu^+\mu^-)}. \tag{12}$$

In the spectator model this should be zero [32], however a deviation is measured to 4.4σ from the SM, which is most significant in low and high q^2 regions. Even more intriguingly A_I for the excited K^* mode is consistent with zero, as expected in the SM.

A resonance at ~ 4190 MeV was observed in the invariant dimuon mass at low kaon recoil, or high q^2, in the decay $B^+ \to K^+\mu^+\mu^-$ [33], where q^2 is the invariant mass of the dimuon system squared, $m^2_{\mu\mu}$. Resonances in this q^2 region are not very well understood, what is known experimentally comes from the BES collaboration [34] where interferences between resonances are accounted for.

The selection is made with $m_{K\mu\mu}$ constrained to the nominal mass of the B in order to increase the resolution of the resonance. A free fit was performed beginning around the $\psi(3770)$ resonance to include a Breit-Wigner resonance which interferes with the non-resonant component of $B^+ \to K^+\mu^+\mu^-$ with a strong phase. Properties of the observed resonance resemble closely those of the $\psi(4160)$ as measured by BES. Therefore another fit was performed with the addition of the $\psi(4160)$ and the $\psi(4040)$ where parameters were allowed to float within their Gaussian uncertainties. The two fit results can be compared in Table 1. [34] To ensure that this resonance is not the $Y(4260)$ [35] a likelihood scan is done in two-dimensions to a single resonance. The resulting profile likelihood is shown in Fig. 7, it shows that the $Y(4260)$ hypothesis is rejected by more than 4σ. This analysis has therefore made the first observation for the decays $B^+ \to \psi(4160)K^+$ and $\psi(4160) \to \mu^+\mu^-$.

Table 1: Results from the fit to the resonance observed in the low recoil region of $B^+ \to K^+\mu^+\mu^-$, where the Unconstrained column is a free fit and that labelled $\psi(4160)$ has parameters allowed to float within the Gaussian uncertainties of measurements by BES [34]. The latter also includes the $\psi(4040)$ state.

		Unconstrained	$\psi(4160)$
$\mathcal{B}$	$[\times 10^{-9}]$	$3.9^{+0.7}_{-0.6}$	$3.5^{+0.9}_{-0.8}$
Mass	[MeV/c^2]	4191^{+9}_{-8}	4190 ± 5
Width	[MeV/c^2]	65^{+22}_{-16}	66 ± 12
Phase	[rad]	-1.7 ± 0.3	-1.8 ± 0.3

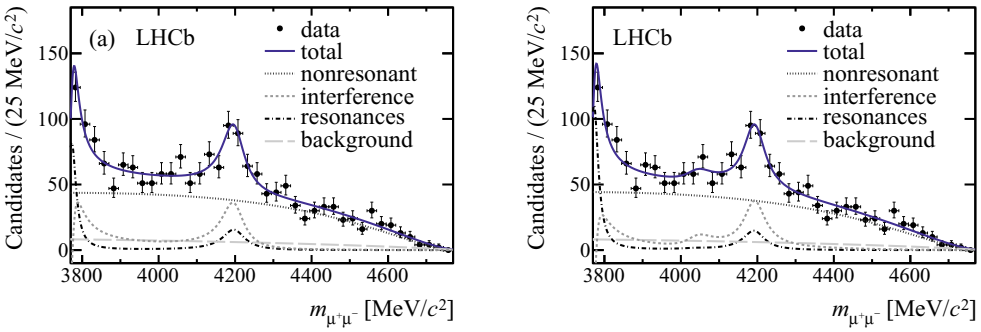

Figure 6: Fits to the dimuon invariant mass spectra where the resonance in the fit is (left) unconstrained, (right) constrained to the BES measurements

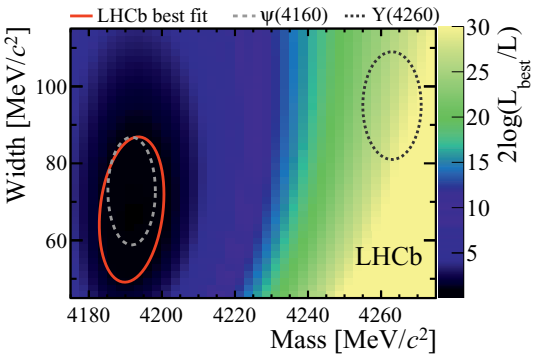

Figure 7: Profile likelihood scan for a single extra resonance interfering with the non-resonant component. It is seen that the LHCb best fit is consistent with the $\psi(4160)$, whereas the hypothesis of the $Y(4260)$ is rejected by more than 4σ.

3.2 Angular analysis of the decay $\mathbf{B^0 \to K^{*0}\mu^+\mu^-}$

The angular analysis of the $B^0 \to K^{*0}\mu^+\mu^-$, where $K^{*0} \to K^+\pi^-$ decay provides information on the helicity structure of the involved amplitudes, which are sensitive to NP contributions.

Three angles describe the decay, they are: ϕ, the angle between the planes formed by the dimuon pair and the daughters of the K^{*0}; θ_ℓ, the angle formed by the flight of the μ^+(μm) and the $B^0(\bar{B}^0)$ meson in the dimuon rest frame; and θ_K, the angle between the flight direction of the kaon and $B^0(\bar{B}^0)$ in the $K^{*0}(\bar{K}^{*0})$ rest frame.

The angular distribution can be written:

$$\begin{aligned}\frac{1}{d\Gamma/dq^2}\frac{d^4\Gamma}{d\cos\theta_K\, d\phi\, dq^2} = \frac{9}{32\pi}\Big[&\tfrac{3}{4}(1-F_L)\sin^2\theta_K + F_{\rm L}\cos^2\theta_K - F_{\rm L}\cos^2\theta_K\cos 2\theta_\ell \\ &+ \tfrac{1}{4}(1-F_{\rm L})\sin^2\theta_K\cos 2\theta_\ell + S_3\sin^2\theta_K\sin^2\theta_\ell\cos 2\phi \\ &+ S_4\sin 2\theta_K\sin 2\theta_\ell\cos\phi + S_5\sin 2\theta_K\sin\theta_\ell\cos\phi \\ &+ S_6\sin^2\theta_K\cos\theta_\ell + S_7\sin 2\theta_K\sin\theta_\ell\sin\phi \\ &+ S_8\sin 2\theta_K\sin 2\theta_\ell\sin\phi + S_9\sin^2\theta_K\sin^2\theta_\ell\sin 2\phi\Big], \end{aligned} \tag{13}$$

where $F_{\rm L}$ is the longitudinal component of the K^{*0} meson and the S_i parameters are functions of Wilson coefficients. It has recently been shown that Eq. 13 can be rewritten with P'_j coefficients [36–40] which have reduced theory uncertainties, where:

$$P'_{j=4,5,6,8} = \frac{S_{i=4,5,7,8}}{\sqrt{F_{\rm L}(1-F_{\rm L})}}. \tag{14}$$

Each P' variable is calculated in 6 bins of q^2 and compare to the SM predictions from Ref. [41]. In all of the q^2 regions for P'_4. P'_6 and P'_8 the experimental results are consistent with theory, Fig 8. However the measurement of P'_5 deviates by 3.7σ from SM predctions in the region $4.3 < q^2 < 8.68\,\mathrm{GeV}^2/c^4$, and deviates by 2.5σ in the the theoretically favoured region ($1 < q^2 < 6\,\mathrm{GeV}^2/c^4$), Fig 8 [42].

4 Summary

Beyond SM physics scenarios often predict observable effects in the flavour sector, particularly in the decays of beauty and charmed mesons. Thus far, new physics has not been observed in the flavour sector despite the higher energies accessible in loop level diagrams through which many of these decays are mediated. Although no observations of NP in the flavour sector have been made many stringent limits have been set which serve to constrain possible NP scenarios.

Sensitive probes for NP are the purely leptonic modes of B^0, B^0_s and D^0 to a dimuon pair, all of which have been analysed by the LHCb collaboration. The first observation of the $B^0_s \to \mu^+\mu^-$ decay has been made and the best limit to date has been set on $B^0 \to \mu^+\mu^-$ in cobination with CMS. A confidence limit has also been set on the branching fraction of the decay $D^0 \to \mu^+\mu^-$.

It is possible that NP could be observed at LHCb directly via lepton flavour violating decays, such as $B^0_{(s)} \to e^\pm\mu^\mp$. A limit on this branching fraction was set, and is consistent with SM predictions. It also

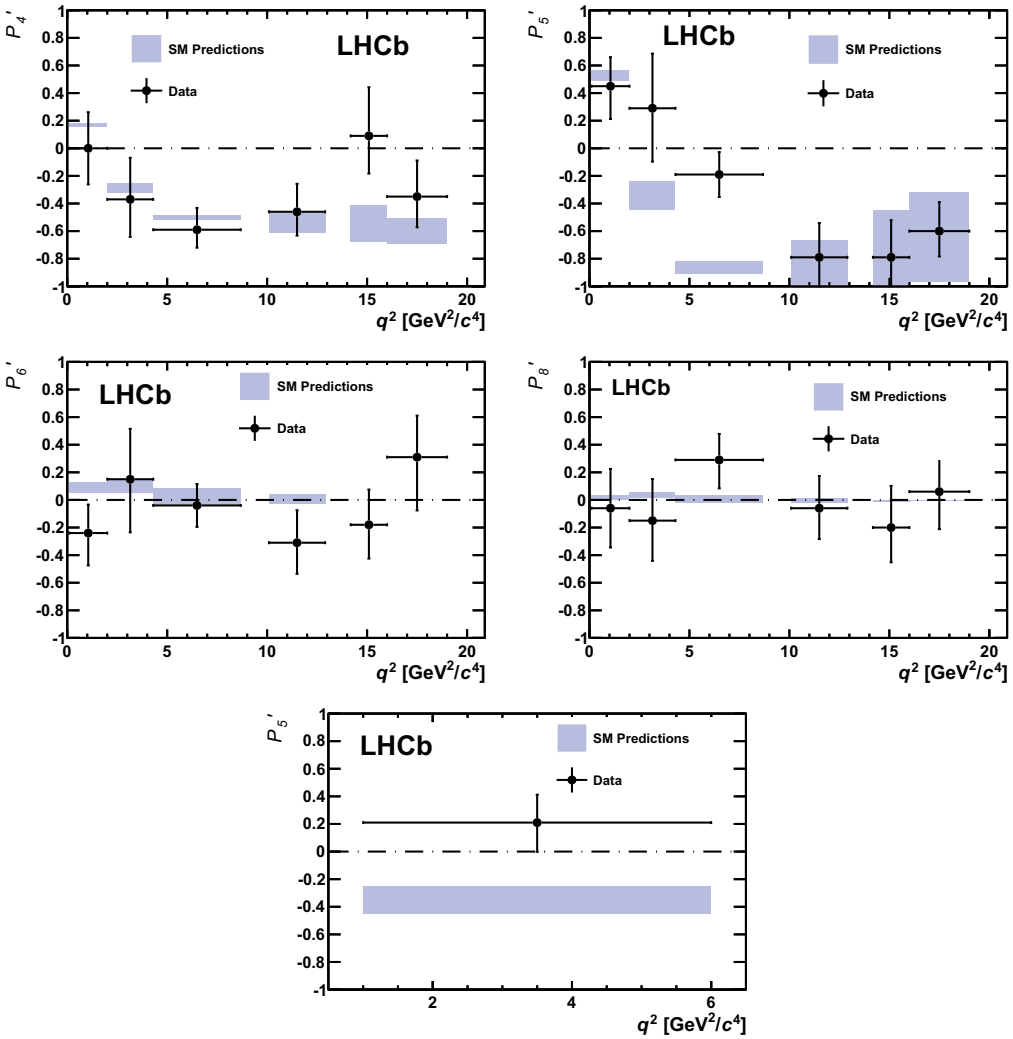

Figure 8: Measurements of the angular observables $P'_{j=4,5,6,8}$ binned in q^2, and the theoretically favoured region of $1 < q^2 < 6\,\mathrm{GeV}^2/c^4$ for P'_5, which is the variable in most tension with the SM.

constrains NP models with LFV, particularly the Pati-Salam model, for which mass constraints on the mediating lepto-quarks are a factor of two higher than previous limits.

The LHCb collaboration have recently observed a new resonance in the dimuon distribution at high q^2 in the decay $B^+ \to K^+\mu^+\mu^-$. This corresponds to the first observation of both $B^+ \to K^+\psi(4160)$ and $\psi(4160) \to \mu^+\mu^-$. Studting resonant structures in the low recoil region of $B^+ \to Kp\mu^+\mu^-$ and how they effect related observables will be an important part of future measurements. Additionally electroweak penguin decays of b-hadrons, coupled with the large data samples from LHCb, open up a whole new area to explore exotic charm states above the open charm threshold.

An angular analysis of the rare electroweak penguin decay $B^0 \to K^{*0}\mu^+\mu^-$ has been performed by the LHCb collaboration using new form factor independent observables.

While experimental results in the flavour sector remain in agreement with theoretical predictions of the SM it must be assumed that either the scale of NP is high, or it mirrors the flavour structure of the SM.

Analyses presented here use the $1\,\text{fb}^{-1}$ collected at $\sqrt{s} = 7\,\text{TeV}$ and some also use the additional $2\,\text{fb}^{-1}$ collected at $\sqrt{s} = 8\,\text{TeV}$. After the current shutdown LHCb will collect $4\,\text{fb}^{-1}$, more than doubling the dataset. Updates with improved sensitivity are therefore to be expected in the near future.

References

[1] R. Aaij et al., Physics Letters B **694**, 209 (2010)
[2] A.A. Alves Jr. et al. (LHCb collaboration), JINST **3**, S08005 (2008)
[3] R. Aaij, J. Albrecht, F. Alessio, S. Amato, E. Aslanides et al. (2012), 1211.3055
[4] A.J. Buras, J. Girrbach, D. Guadagnoli, G. Isidori, Eur.Phys.J. **C72**, 2172 (2012), 1208.0934
[5] R. Aaij et al. (LHCb collaboration), Phys. Rev. Lett. **108**, 231801 (2012), 1203.4493
[6] A. Abulencia et al. (CDF Collaboration), Phys.Rev.Lett. **95**, 221805 (2005), hep-ex/0508036
[7] R. Aaij et al. (LHCb collaboration), Phys. Rev. Lett. **111**, 101805 (2013), 1307.5024
[8] R. Aaij et al. (LHCb collaboration), JHEP **04**, 1 (2013), 1301.5286
[9] A.L. Read, Journal of Physics G: Nuclear and Particle Physics **28**, 2693 (2002)
[10] S. Chatrchyan et al. (CMS Collaboration) (2013), 1307.5025
[11] *Combination of results on the rare decays* $B^0_{(s)} \to \mu^+\mu^-$ *from the CMS and LHCb experiments* (2013), CMS-PAS-BPH-13-007, LHCb-CONF-2013-012
[12] F. Beaujean, C. Bobeth, D. van Dyk (2013), 1310.2478
[13] W. Altmannshofer, D.M. Straub, JHEP **1208**, 121 (2012), 1206.0273
[14] W.S. Hou, M. Kohda, F. Xu, Phys.Rev. **D87**, 094005 (2013), 1302.1471
[15] G.W.S. Hou (2013), 1307.2448
[16] G. Burdman, E. Golowich, J. Hewett, S. Pakvasa, Phys. Rev. D **66**, 014009 (2002)
[17] H. Guler et al. (The Belle Collaboration), Phys. Rev. D **81**, 091102 (2010)
[18] E. Golowich, J. Hewett, S. Pakvasa, A.A. Petrov, Phys. Rev. D **79**, 114030 (2009)
[19] R. Aaij et al. (LHCb collaboration), Phys. Lett. **B725**, 15 (2013), 1305.5059
[20] A. Ilakovac, Phys. Rev. D **62**, 036010 (2000)
[21] R. Diaz, R. Martinez, C. Sandoval, The European Physical Journal C - Particles and Fields **46**, 403 (2006)
[22] S. Kovalenko, I. Schmidt, Phys.Lett. **B562**, 104 (2003), hep-ph/0210187
[23] J.C. Pati, A. Salam, Phys. Rev. **D10**, 275 (1974), erratum-ibid. **D11** (1975) 703
[24] G. Aad et al. (ATLAS Collaboration), JHEP **1306**, 033 (2013), 1303.0526
[25] G. Aad et al. (ATLAS Collaboration), Phys.Lett. **B709**, 158 (2012), 1112.4828
[26] G. Aad et al. (ATLAS Collaboration), Eur.Phys.J. **C72**, 2151 (2012), 1203.3172
[27] S. Chatrchyan et al. (CMS Collaboration), JHEP **1212**, 055 (2012), 1210.5627
[28] S. Chatrchyan et al. (CMS Collaboration), Phys.Rev. **D86**, 052013 (2012), 1207.5406
[29] S. Chatrchyan et al. (CMS Collaboration), Phys.Rev.Lett. **110**, 081801 (2013), 1210.5629
[30] R. Aaij et al. (LHCb collaboration) (2013), to appear in Phys. Rev. Lett., 1307.4889
[31] R. Aaij et al. (LHCb collaboration), JHEP **07**, 133 (2012), 1205.3422

[32] P. Ball, R. Zwicky, Phys.Rev. **D71**, 014029 (2005), hep-ph/0412079
[33] R. Aaij et al. (LHCb collaboration) (2013), to appear in Phys. Rev. Lett., 1307.7595
[34] M. Ablikim et al. (The BES Collaboration), Physics Letters B **660**, 315 (2008)
[35] J. Beringer et al. (Particle Data Group), Phys. Rev. **D86**, 010001 (2012)
[36] D. Becirevic, E. Schneider, Nucl.Phys. **B854**, 321 (2012), 1106.3283
[37] J. Matias, F. Mescia, M. Ramon, J. Virto, JHEP **1204**, 104 (2012), 1202.4266
[38] F. Kruger, J. Matias, Phys.Rev. **D71**, 094009 (2005), hep-ph/0502060
[39] U. Egede, T. Hurth, J. Matias, M. Ramon, W. Reece, JHEP **0811**, 032 (2008), 0807.2589
[40] C. Bobeth, G. Hiller, D. van Dyk, JHEP **07**, 067 (2011), 1105.0376
[41] S. Descotes-Genon, T. Hurth, J. Matias, J. Virto, JHEP **1305**, 137 (2013), 1303.5794
[42] R. Aaij et al. (LHCb collaboration) (2013), submitted to Phys. Rev. Lett., 1308.1707